Acta Biomaterialia 24 (2015) 279–285

Contents lists available at ScienceDirect

Acta Biomaterialia

journal homepage: www.elsevier.com/locate/actabiomat

Full length article

Therapeutic efficacy of doxorubicin delivery by a CO_2 generating liposomal platform in breast carcinoma

Hee Dong Han [a,1], Ye Won Jeon [b,1], Ho Jin Kwon [b,c], Hat Nim Jeon [a], Yeongseon Byeon [a], Chong Ock Lee [b], Sun Hang Cho [b], Byung Cheol Shin [b,c,*]

[a] Department of Immunology, School of Medicine, Konkuk University, 268 Chungwondaero, Chungju-Si, Chungcheongbuk-Do 380-701, South Korea
[b] Bio/Drug Discovery Division, Korea Research Institute of Chemical Technology, 141 Gajeong-ro, Yuseong-gu, Daejeon 305-600, South Korea
[c] Medicinal and Pharmaceutical Chemistry, University of Science and Technology, Yuseong, Daejeon 305-350, South Korea

ARTICLE INFO

Article history:
Received 10 March 2015
Received in revised form 21 May 2015
Accepted 15 June 2015
Available online 20 June 2015

Keywords:
Liposome
Doxorubicin
Cancer
Gas generation
Breast cancer

ABSTRACT

Drug delivery using thermosensitive liposomes (TSL) has significant potential for tumor drug targeting and can be combined with local hyperthermia to trigger drug release. Although TSL-mediated drug delivery can be effective by itself, we developed doxorubicin (DOX)-containing CO_2 bubble-generating TSL (TSL-C) that were found to enhance the antitumor effects of DOX owing to the synergism between burst release of drug and hyperthermia-induced CO_2 generation. An ultrasound imaging system was used to monitor hyperthermia-induced CO_2 generation in TSL-C and the results revealed that hyperthermia-induced CO_2 generation in TSL-C led to increased DOX release compared to that observed for non-CO_2-generating TSL. Moreover, TSL-C significantly inhibited the tumor growth in MDA-MB-231 tumor-bearing mice compared to TSL ($p < 0.004$). Taken together, we demonstrated that the TSL-C platform increased the therapeutic efficacy of cancer chemotherapy and showed the applicability of this approach to increase drug release within the tumor microenvironment. As a novel and highly effective drug delivery platform, TSL-C has great potential for use in a broad range of applications for the treatment of various human diseases.

Statement of Significance

We have developed a novel method for drug release from liposomes by gas (CO_2) generation in tumor microenvironment. In addition, we demonstrate therapeutic efficacy in breast carcinoma. CO_2-generated liposomal doxorubicin is a novel and highly attractive delivery system for anticancer drug with the potential for broad applications in human disease.

1. Introduction

Liposome-based anticancer drug delivery systems have great potential for cancer chemotherapies [1,2]. Although liposomes provide a promising chemotherapeutic strategy, their use in clinical trials for controlled drug release has been limited. To overcome the limitations associated with the use of liposomes, surface modification by polymers [3,4] and external stimulation-triggered drug release strategies [5] have been employed to develop advanced liposomal formulations, such as pH- [6,7], ultrasound- [8,9], and light-sensitive liposomes [10,11], for increased drug release at the target site. Although advanced liposomal systems have been developed to increase drug release within tumor tissue, the factors determining the optimum formulation and control of drug release for effective chemotherapy are not well understood. These issues have increased the need for novel and improved liposomal systems to overcome the existing therapeutic limitations.

In particular, thermosensitive liposomes (TSL) have attracted considerable attention owing to their ability to enhance drug release at the target site [12,13]. Effective drug release from TSL in tumor tissue increases the therapeutic efficacy. To increase drug release from liposomes, we encapsulated both ammonium bicarbonate (NH_4HCO_3) and doxorubicin (DOX) into TSL to generate CO_2 bubbles in response to external hyperthermia [14]. NH_4HCO_3 is widely used as a CO_2 raising agent in the food industry for the generation of gas bubbles in baked goods, and it can quickly

* Corresponding author at: Bio/Drug Discovery Division, Korea Research Institute of Chemical Technology, 141 Gajeong-ro, Yuseong-gu, Daejeon 305-600, South Korea.
E-mail address: bcshin@krict.re.kr (B.C. Shin).
[1] These authors contributed equally to this work.

http://dx.doi.org/10.1016/j.actbio.2015.06.019
1742-7061/

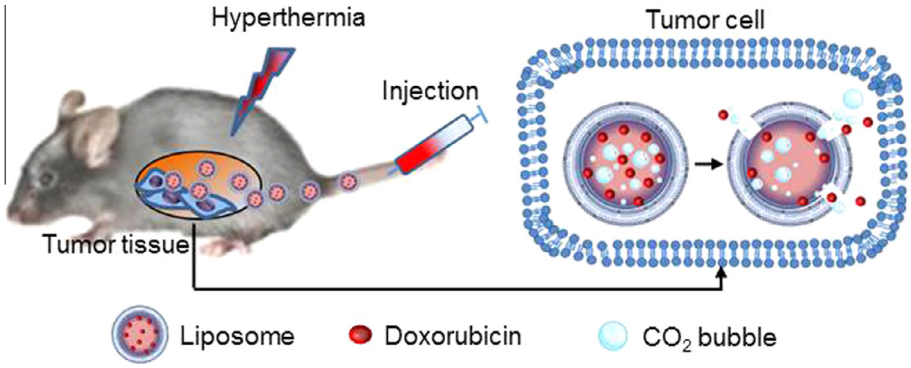

Fig. 1. Schematic illustration of hyperthermia-induced DOX release from CO_2-generating liposomal platform.

decompose to generate CO_2 bubbles at temperatures above 40 °C [15,16]. Thus, we postulated that external hyperthermia-induced gas generation in liposomes could promote drug release by increasing liposomal membrane destabilization (Fig. 1) [17]. These findings motivated us to determine whether CO_2 bubble generation in liposomes could promote drug release, leading to an increased therapeutic efficacy.

Here, we present a novel liposomal DOX platform as a cancer chemotherapeutic agent designed to increase drug release at the tumor site by CO_2 bubble generation. Furthermore, the therapeutic efficacy of DOX released from CO_2-generating TSL (TSL-C) was evaluated in the presence or absence of hyperthermia. This study aimed to provide a significant conceptual advance in the understanding of liposomal delivery systems for cancer chemotherapy.

2. Materials and methods

2.1. Materials

Dipalmitoylphosphatidyl-choline (DPPC), monostearoylpho sphatidylcholine (MSPC), and 1,2-distearoyl-*sn*-glycero-3-phospho ethanolamine-N-[methoxy(polyethylene glycol)-2000] (DSPE-mPEG-2000) were purchased from Avanti Polar Lipids Inc. (Alabaster, AL, USA). Doxorubicin hydrochloride (DOX), citric acid, 4-(2-hydroxyethyl)-1-piperazineethane sulfonic acid (HPES), Sephadex® G-50, and ammonium bicarbonate (NH_4HCO_3) were purchased from Sigma-Aldrich (St. Louis, MO, USA). Fetal bovine serum (FBS), penicillin–streptomycin, and Dulbecco's modified Eagle's medium (DMEM) were purchased from Gibco BRL/Life Technologies (New York, NY, USA). All other materials were of analytical grade and used without further purification.

2.2. Preparation of TSL or TSL-C

TSL were prepared by thin-lipid film hydration and the sequential extrusion method [18,19]. The encapsulation of DOX in the aqueous core of the liposomes was achieved by the remote loading method using an ammonium sulfate transmembrane gradient. The lipid compositions and molar ratios for TSL preparation were DPPC:MSPC:DSPE-mPEG-2000 = 21.6:2.6:1.0. These lipids were dissolved in 3 ml of chloroform to give a total lipid concentration of 25.2 mM and dried to a thin film using a rotary evaporator under a vacuum. The film was hydrated with 3 ml of 300 mM ammonium sulfate solution and the resulting liposome suspension was extruded sequentially 5 times through polycarbonate membrane filters (Whatman, Piscataway, NJ, USA) with a pore size of 200 and 100 nm using a high-pressure extruder (Northern Lipids Inc., Burnaby, Canada). Free ammonium sulfate was removed by dialysis in distilled water for 48 h at 4 °C using a cellulose dialysis tube (MWCO, 12,000–14,000; Viskase Co., Darien, IL, USA). DOX solution (2 mg/ml) was added to the liposomal suspension (1:1 v/v) and incubated for 2 h at 25 °C. The mixture was then dialyzed for 48 h at 4 °C to remove the free DOX.

The CO_2-generating TSL-C were also prepared using the thin-lipid film hydration method with minor modifications of the TSL preparation. The experimental procedure for the preparation of TSL-C was similar to that described above. For TSL-C, the dried lipid film was hydrated with 3 ml of 300 mM citric acid buffer solution (pH 4). DOX solution (2 mg/ml) containing 253 mM of NH_4HCO_3 was added to the liposomal solution (1:1 v/v) and incubated for 2 h at 25 °C. The mixture was dialyzed for 48 h at 4 °C to remove the free DOX and NH_4HCO_3. The TSL and TSL-C were stored at 4 °C until use.

The particle size and zeta potential of liposomes were measured by laser light scattering using a particle size analyzer (ELS-8000, Outskate, Japan). The loading efficiency of DOX into liposomes was measured by UV–vis spectrophotometry (UV-mini, Shimadzu, Japan) at wavelength of 490 nm after dissolution of the liposomes in a chloroform–methanol mixture (8:2, v/v) [19]. In addition, morphologies of TLS-C after both DOX and NH_4HCO_3 encapsulation were monitored by cryogenic transmission electron microscopy (cryo-TEM, Tecnai G2 Spirit, FEI Company, Hillsboro, OR, USA).

2.3. Intracellular uptake of liposomes into tumor cells

The breast cancer cell line, MDA-MB-231, was maintained and propagated in DMEM supplemented with 10% fetal bovine serum and 0.1% gentamicin sulfate (Gemini Bioproducts, Calabasas, CA). All *in vitro* and *in vivo* experiments were conducted when cells were 70–80% confluent. The intracellular uptake of TSL or TSL-C was observed using flow cytometry (FACScan, Becton Dickinson) with CELLQuest software (Becton Dickinson Immunocytometry System, Mountain View, CA). The MDA-MB-231 cells were plated in a 6-well plate at a density of 2×10^5 cells per well and cultured in DMEM at 37 °C. This culture medium was replaced with 2 ml per well of culture medium containing liposomal solutions. The cells were incubated with liposomes for 1 h at 37 °C in a 5% CO_2 incubator. After incubation, the cells were washed 3 times with phosphate-buffered saline (PBS). The intracellular uptake of liposomes in MDA-MB-231 cells was monitored by flow cytometry, and the morphologies of tumor cells containing TSL-C were observed by confocal microscopy (Carl Zeiss, LSM 710, Germany).

2.4. Observation of CO_2 generation in TSL-C by ultrasound imaging

The generation of CO_2 in TSL-C was monitored using an ultrasound imaging system with a 7 MHz transducer (TELEMED, Lithuania). The TSL and TSL-C were placed in round bottomed

tubes, which were warmed to 37 °C, 42 °C, and 45 °C. The CO_2 generation was automatically displayed by B-mode anatomic images.

2.5. Drug release from TSL-C

Temperature-sensitive drug release from liposomes was measured as a function of temperature and incubation time. The liposome suspensions were diluted with PBS (pH 7.4) at a ratio of 1:4 (v/v). The release of DOX from liposomes was measured using a UV–vis spectrophotometer (UV-mini) at a wavelength of 490 nm. The percentage of DOX released from the liposomes was calculated according to the formula [8]:

$$\text{Drug release } (\%) = (F_t - F_0)/(F_{max} - F_0) \times 100$$

where F_t was the DOX intensity of the liposome, F_0 was the initial background DOX intensity of the liposome, and F_{max} was the intensity of DOX in the liposomes after the dissolution of DOX-loaded liposomes in the organic solvent mixture consisting of chloroform and methanol (4:1 v/v). The drug-release test was performed using 3 independent samples of each liposomal formulation.

2.6. Cytotoxicity of TSL-C

The cytotoxicity of the TSL and TSL-C with or without hyperthermia was determined by MTT assay [20]. The MDA-MB-231 cells were seeded into 96-well plates at a density of 1×10^3 cells per well and cultured at 37 °C in 5% CO_2 for 2 h in DMEM containing liposomes. After incubation, the plates were heated to 42 °C for 2 min to trigger CO_2 generation in TSL-C. Thereafter, the plates were washed with PBS, the medium was replaced, and the cells were incubated for 48 h. The absorbance was measured at 590 nm using a microplate reader (EL808, Bio-Tek, Ins., USA).

2.7. Cell death assay for TSL-C

The relative percentage of necrotic and apoptotic cells was assessed using the Annexin V-FITC apoptosis Detection Kit-1 (BD Pharmingen, San Diego, CA) according to the manufacturer's protocol. Briefly, control, TSL, and TSL-C were incubated with MDA-MB-231 cells for 30 min at room temperature to induce intracellular delivery of liposomes. After that, the plates were heated to 42 °C for 10 min to generate CO_2 within TSL-C. Thereafter, the cells were incubated for 24 h. After incubation, the cells were washed twice in PBS, and the pellet was resuspended in annexin V binding buffer at a concentration of 10^6 -cells/ml. Annexin-propidium iodide (PE) and 7-AAD (7-amino-actinomycin D) were added (5 μl of each per 10^5 cells). Samples were mixed gently and incubated for 15 min at room temperature in the dark before flow cytometry analysis [21].

2.8. Antitumor efficacy

Female athymic nude mice (NCr-nu) were purchased from Orient Co. (Seoul, South Korea). All mouse studies were approved by the Konkuk University Institutional Animal Care and Use Committee (Ref. No. KU14009). The mice used for *in vivo* experiments were 5–6 weeks old. To produce tumors, MDA-MD-231 (5×10^5 cells per 0.05 ml HBSS) cells were injected into the subcutaneous (s.c.) of mice. Mice ($n = 6$ per group) were monitored daily for adverse effects of therapy and were sacrificed when any of the mice seemed moribund.

To assess tumor growth, treatment began 1 week after s.c. injection of MDA-MB-231 cells into mice. TSL-C was given once weekly at a dose of 5 mg DOX/kg body weight through intravenous (i.v.) injection. Four hours after i.v. injection of TSL-C, a near infrared (NIR) laser as a heat source for hyperthermia was irradiated at 1.75 W/cm^2 for 3 min. Treatment continued until mice became moribund (typically 3–4 weeks). Mouse weight, tumor volume, and tumor weight were recorded. The individuals who performed the necropsies, tumor collections, and tissue processing were blinded to the treatment group assignments. Tissue specimens were fixed with formalin [22].

2.9. Immunohistochemical staining

Immunohistochemical (IHC) analysis was performed on tumor tissue from mice treated with i.v. injection of TSL-C. Procedures for IHC analysis of cell proliferation (Ki67) and cell apoptosis (caspase 3 antibody) were performed as described previously [22]. All of these analyses were recorded in 4 random fields for each slide. The quantification of apoptotic cells was calculated by the number of apoptotic cells in 4 random fields. All staining was quantified by 2 investigators in a blinded fashion.

2.10. Statistical analysis

Differences in continuous variables were analyzed by Student's *t*-test for comparing two groups and ANOVA was performed to compare differences between multiple groups. For values that were not normally distributed, the Mann–Whitney rank sum test was used. The statistical package for the Social Sciences (SPSS, Inc.) was used for all statistical analyses. A p value of <0.05 was considered statistically significant.

3. Results

3.1. Characteristics of liposomes

We first confirmed the physical properties of the liposomes (Fig. 2). The mean particle size of TSL and TSL-C were 100.63 ± 3.69 nm and 103.2 ± 5.91 nm, respectively, and the surface charge was −10 mV (Fig. 2A and B). In addition, loading efficiency of DOX into TSL was over 94.76%, and the concentration of DOX was 880.50 μg/ml, while the loading efficiency of TSL-C was 81.03% and the concentration was 811.78 μg/ml (Fig. 2C and D). The loading efficiency of DOX into liposomes was dependent on the sulfate or citrate gradient [23]. The loading efficiency of DOX into TSL using an ammonium salt gradient was higher than that of TSL-C when a sodium salt gradient was used. Although the loading efficiency of TSL was higher, there were no significant differences between the particle size and surface charge of TSL and TSL-C, demonstrating that NH_4HCO_3 encapsulation did not affect the physicochemical properties of the liposomes.

3.2. Intracellular delivery of TSL or TSL-C in MDA-MB-231 cells

We next assessed the intracellular uptake of liposomes by flow cytometry and confocal microscopy (Fig. 3). Flow cytometry analysis indicated that both TSL and TSL-C exhibited highly efficient and dose-dependent intracellular delivery, as compared to the control (Fig. 3A and B). In addition, confocal microscopy analysis showed that TSL-C uptake by tumor cells was consistent with the flow cytometry data (Fig. 3C).

3.3. CO_2-generation and release of DOX from TSL-C

Prior to testing DOX release from liposomes, we monitored hyperthermia-induced CO_2 generation in TSL-C using an ultrasound imaging system. While TSL showed no bubble generation, TSL-C showed CO_2 bubble generation at 42 °C (Fig. 4A). We next observed the morphologies of TSL-C before and after hyperthermia

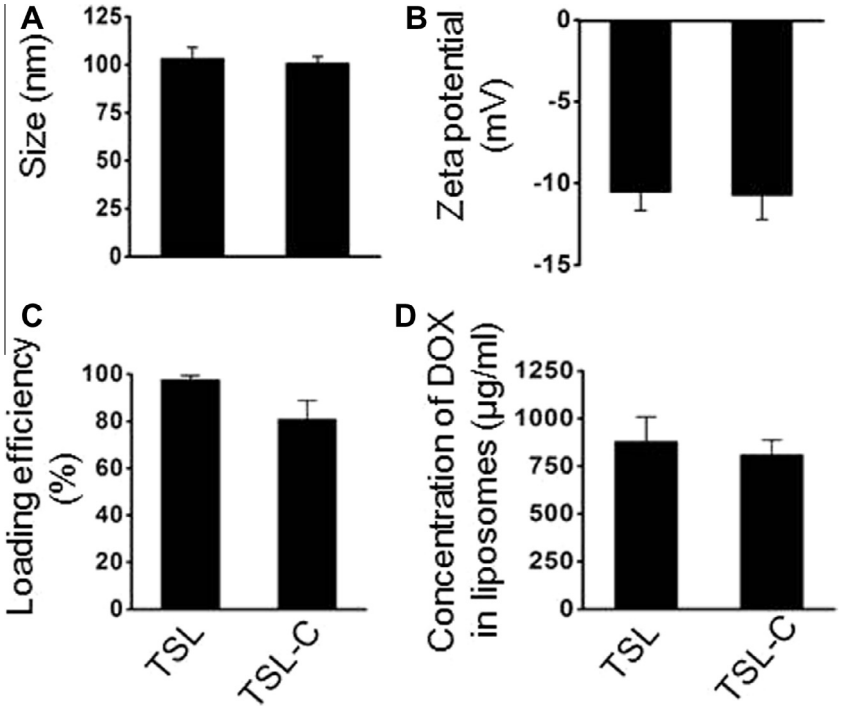

Fig. 2. Physical properties of TSL and TSL-C. (A) Size and (B) zeta potential of liposomes were measured by light scattering with a particle size analyzer. (C) Loading efficiency and (D) concentration of DOX into liposomes were determined by fluorescence spectrophotometry. The data are presented as the mean ± S.D. (n = 3).

to investigate whether CO_2 generation promoted liposomal membrane destabilization (Fig. 4B). Notably, we observed a black bar in the center of TSL-C, which clearly indicated DOX encapsulation into liposomes. However, after hyperthermia, the liposomal membrane destabilized and the size of TSL-C decreased, possibly triggering a release of DOX from the liposomes. This data demonstrated that CO_2 generation by hyperthermia in TSL-C promoted DOX release and membrane destabilization.

The release of DOX from TSL and TSL-C was measured at various temperatures and times (Fig. 4C and D). At normal body temperature of 37 °C, TSL and TSL-C showed a limited increase in DOX release, whereas drug release from TSL-C greatly increased in the hyperthermia region (40–42 °C) compared to TSL (Fig. 4C), indicating that TSL-C was safe in circulation after injection at body temperature. Moreover, this data also clearly indicated that CO_2 generation in TSL-C promoted DOX release in hyperthermia conditions. In addition, drug release was measured at the same incubation in the presence or absence of hyperthermia (Fig. 4D). Although TSL with hyperthermia resulted in an increased drug release (60%) within 4 min at 42 °C, TSL-C with hyperthermia showed a much higher increase in drug release (80%) within 1 min at 42 °C, indicating that hyperthermia-induced CO_2 generation within liposomes significantly promoted DOX release.

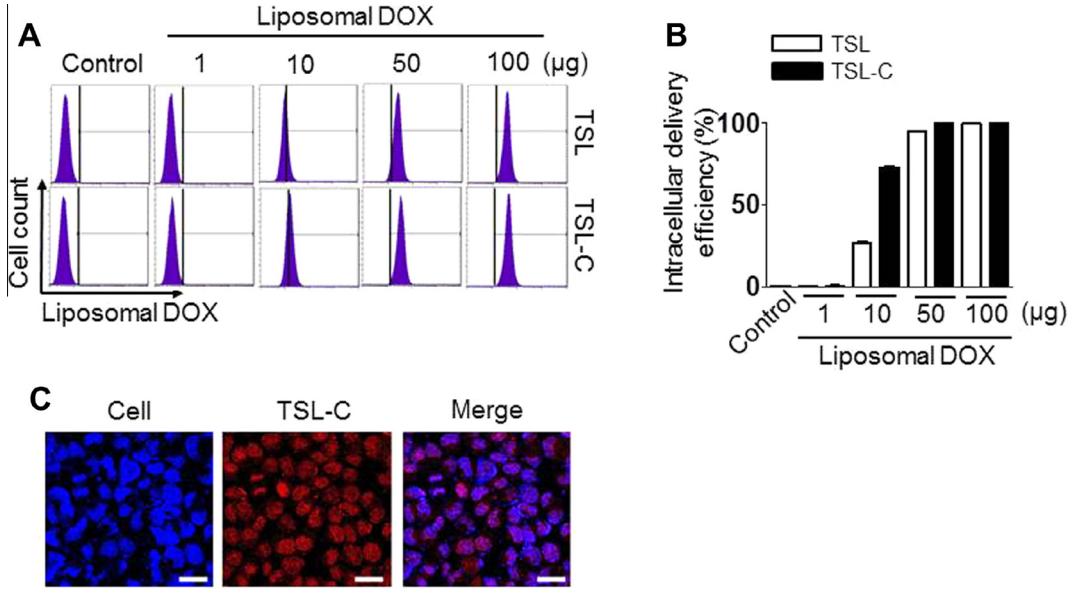

Fig. 3. Intracellular uptake of liposomes. (A and B) Flow cytometric assessment of the intracellular delivery of liposomes in MDA-MB-231 tumor cells incubated with TSL or TSL-C. (C) The intracellular uptake of liposomes in tumor cells was observed by confocal microscopy. Blue: nuclei, Red: DOX, Scale bar: 20 μm.

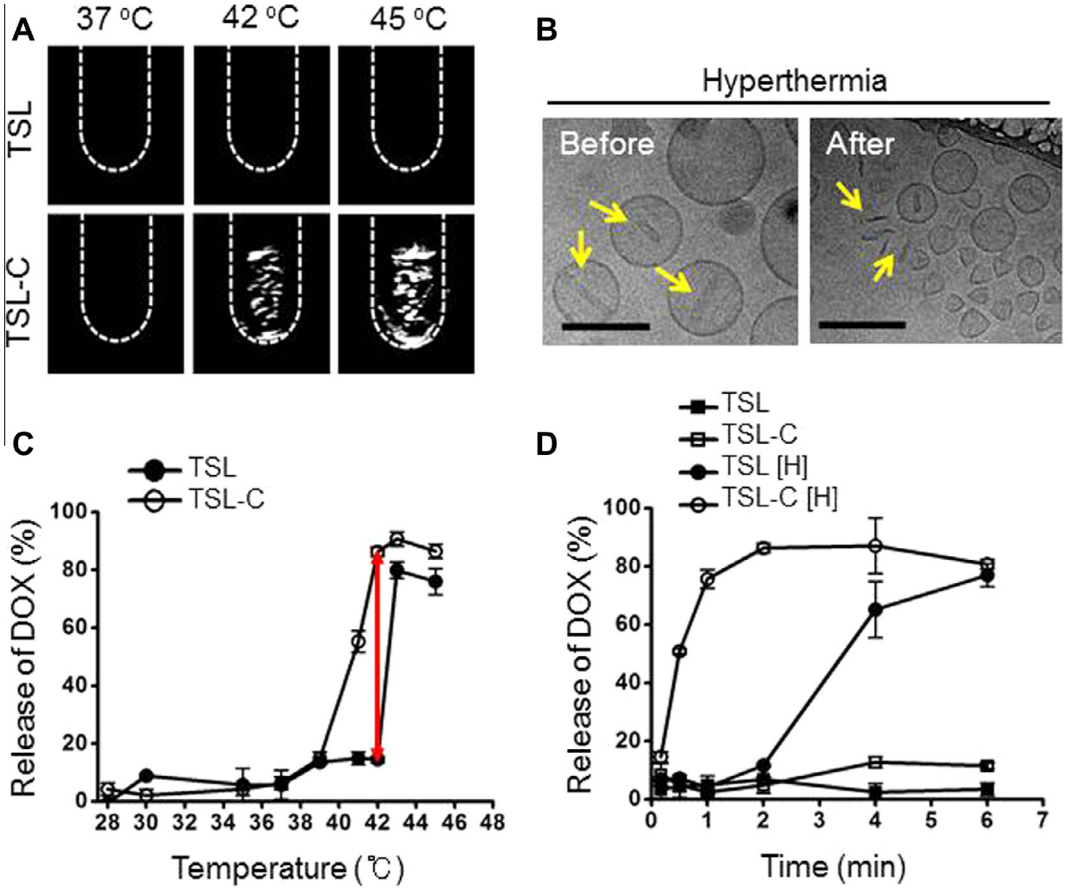

Fig. 4. Release of DOX from liposomes. (A) The generation of CO_2 bubbles in TSL-C was monitored using an ultrasound imaging system with a 7 MHz transducer. (B) Morphologies of TSL-C encapsulated with DOX and NH_4HCO_3 before and after hyperthermia were monitored by cryogenic transmission electron microscopy. Scale bar: 100 nm. (C) Release of DOX from liposomes at various temperatures and (D) times. [H] indicates that the liposomes were exposed to hyperthermia at 42 °C. The data are presented as the mean ± S.D. (n = 3).

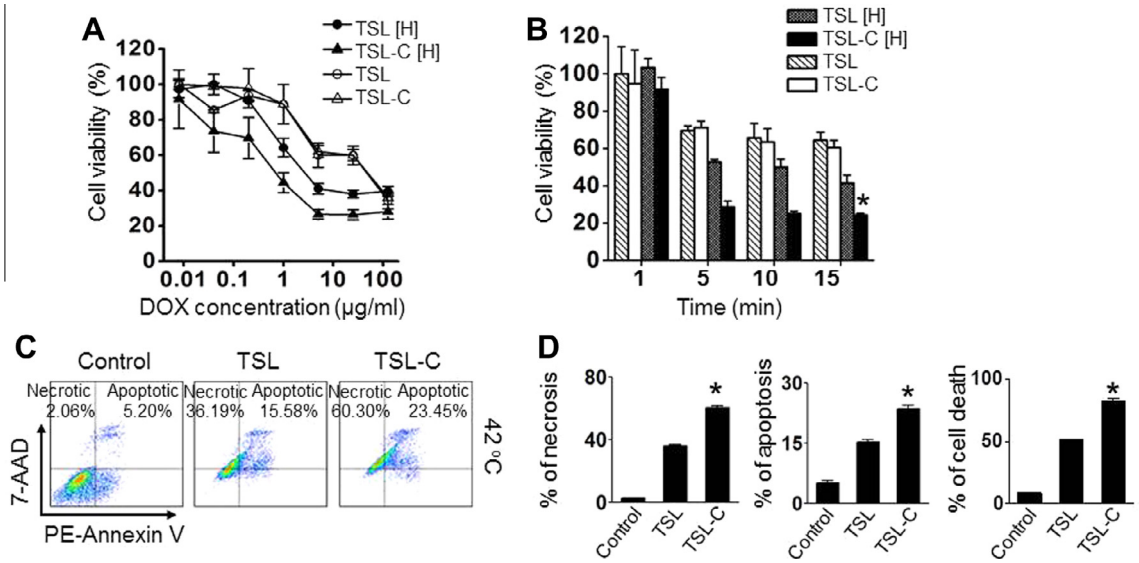

Fig. 5. Cell death assays. (A and B) Cytotoxicity of TSL and TSL-C containing DOX towards MDA-MB-231 cells with or without hyperthermia (42 °C). [H] indicates hyperthermia treatment at 42 °C. (C and D) Cell death assay of MDA-MB-231 cells exposed to TSL or TSL-C. The relative percentage of necrotic and apoptotic cells was assessed by 7-AAD and annexin V double staining. Afterwards, necrosis and apoptosis were determined by flow cytometry. The data are presented as the mean ± S.D. $^{*}p < 0.05$.

3.4. Cytotoxicity of liposomes

To confirm whether cytotoxicity increased following CO_2-mediated DOX release from TSL-C, we determined the *in vitro* cytotoxicity and apoptosis induced by TSL and TSL-C with or without hyperthermia by MTT assay and flow cytometry analysis (Fig. 5). The TSL-C with hyperthermia was more cytotoxic towards MDA-MB-231 cells than either TSL or TSL-C without

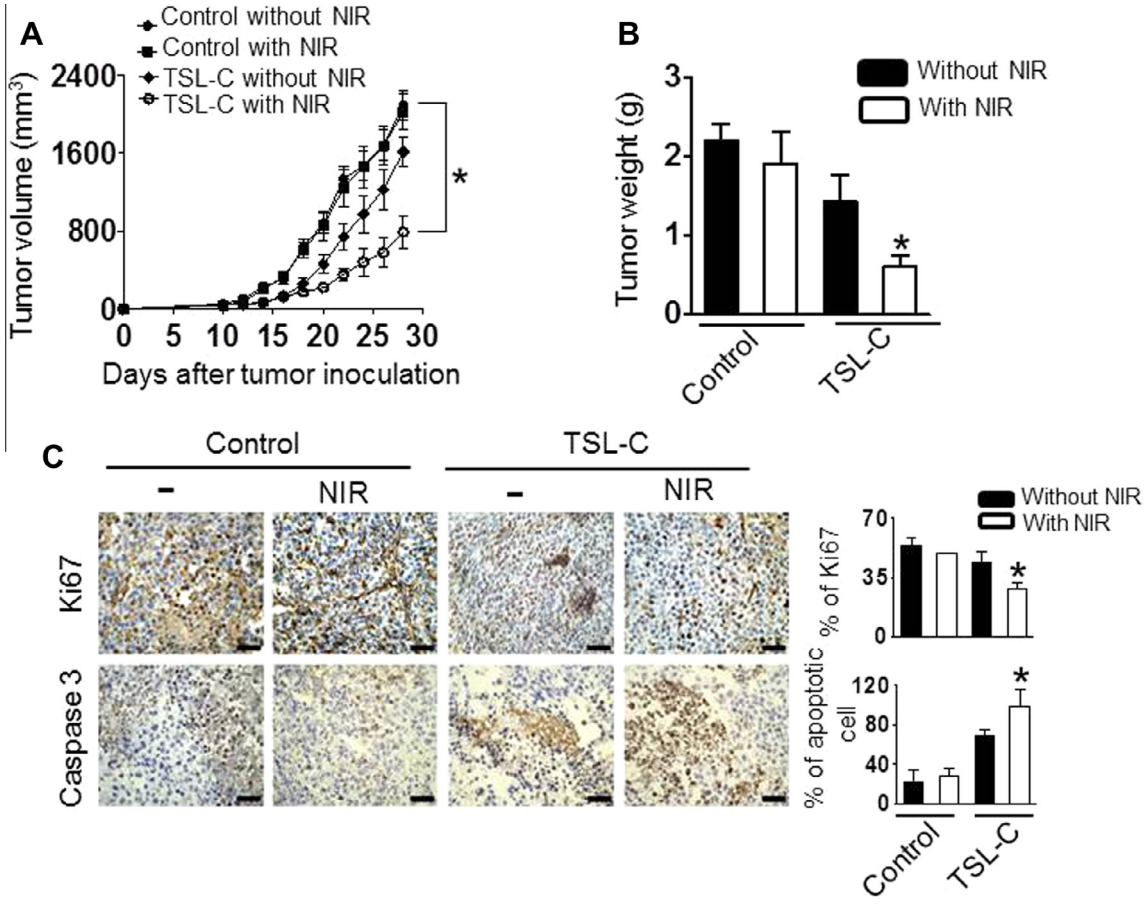

Fig. 6. Antitumor effect of TSL-C in MDA-MB-231 tumor bearing mice. (A) Tumor growth and (B) tumor weight were monitored. Treatment was started 1 week after subcutaneous injection of MDA-MB-231 cells (5×10^5) into mice ($n = 6$). TSL-C was given by i.v. injection once per week at a dose of 5 mg/kg body weight. A NIR (near infrared) laser was used as a local heat source. Four hours after TSL-C injection, the tumor was exposed to NIR at 1.75 W/cm^2 (42 °C) for 3 min. Treatment was continued until the mice in any group became moribund. Error bars represent the standard error of the mean s.e.m. $^*p < 0.004$. (C) Immunohistochemical analyses of cell proliferation (Ki67) and caspase 3 were performed on tumor tissues following treatment with TSL-C with or without hyperthermia. All of these analyses were recorded in 4 random fields for each slide. Error bars represent s.e.m. $^*p < 0.05$. Bar: 50 μm.

hyperthermia ($^*p < 0.05$) (Fig. 5A and B). The higher cytotoxicity of TSL-C with hyperthermia clearly indicated that their drug release increased owing to CO_2 generation.

We next assayed necrosis and apoptosis analysis using flow cytometry (Fig. 5C and D). Cell necrosis increased significantly in the presence of TSL-C compared to TSL at 42 °C ($^*p < 0.01$, Fig. 5C and D). CO_2 bubble generation in liposomes amplified the cavitation effect [15]. This cavitation effect on lysosomes can mechanically disrupt the cell membranes, resulting in increased necrosis [15]. In addition, apoptosis also increased in tumor cells treated with TSL-C owing to burst release of DOX from liposomes. Overall, cell death significantly increased in the presence of TSL-C compared to TSL (Fig. 5D).

3.5. Therapeutic efficacy of TSL-C

To determine the effectiveness of potential therapeutic efficacy of TSL-C, we utilized breast carcinoma MDA-MB-231 cells, which play a significant role in cell invasion, leading to increased metastasis of cancer cells [24]. In addition, breast cancer treatment using a combination therapy involving external hyperthermia treatment is promising. Seven days following s.c. injection of tumor cells into the mice, the animals were randomly allocated to the following groups ($n = 6$ mice/group): (1) control without NIR, (2) control with NIR, (3) TSL-C without NIR, and (4) TSL-C with NIR. All mice were sacrificed when animals in any group appeared moribund. TSL-C without NIR resulted in significant inhibition of tumor growth compared to the control without NIR (36% reduction; $p < 0.004$). Notably, the combination of TSL-C with NIR showed the greatest inhibition of tumor growth compared to the control without NIR (72% reduction, $p < 0.002$) and TSL-C without NIR (57% reduction, $p < 0.028$; Fig. 6A and B). There were no differences in total body weight, feeding habits, or behavior between the groups, suggesting that there were no overt toxicities related to therapy.

To determine the potential mechanisms underlying the efficacy of TSL-C with NIR therapy in tumor tissues, we examined the tumors for markers of cell proliferation (Ki67) and apoptosis (caspase 3). TSL-C with NIR significantly inhibited cell proliferation ($p < 0.003$ *vs* control without NIR; $p < 0.03$ *vs* TSL-C without NIR) and increased apoptosis ($p < 0.001$ *vs* control without NIR; $p < 0.04$ *vs* TSL-C without NIR) (Fig. 6C).

4. Discussion

We demonstrate here that a novel liposomal CO_2-generating DOX delivery platform combined with hyperthermia leads to potent anti-tumor efficacy in breast carcinoma. This approach has broad utility for enhancing the therapeutic effects on tumor cells. Hyperthermia-induced CO_2 generation within liposomes resulted in effective drug release and could be applied to multiple cancer models achieve high therapeutic efficacy.

The therapeutic efficacy at a target tissue is highly associated with the characteristics of drug release from liposomes. Conventional TSL are capable of temperature-sensitive drug release at the target site. Although TSL formulations are capable for controlled drug release, liposomal systems still need to increase therapeutic efficacy for sufficient drug release at the tumor site to increase therapeutic efficacy [12]. Therefore, to increase drug release from liposomes, stimuli-responsive strategies have been developed [5]. Among them, CO_2 generating liposomes were developed for drug burst release from liposomes in response to hyperthermia or ultrasound irradiation [14,15]. The CO_2 generating liposomal platform has been applied to the treatment of diverse diseases such as cancer, demonstrating the system's therapeutic efficacy [1,17]. Here, we developed an advanced TSL-C system by encapsulating both ammonium bicarbonate (NH_4HCO_3) and DOX into the liposomes, facilitating drug release by CO_2 generation under hyperthermic conditions. This CO_2 generating liposomal platform may be attractive for many biomedical applications when combined with local hyperthermia at the target site, including administration of treatment agents for diseases.

In summary, the TSL-C system has demonstrated great potential for providing increased drug release at tumor sites in cancer chemotherapy and will be useful as a drug delivery system for treating many other diseases. In addition, the use of the TSL-C delivery system can be useful in a range of hyperthermia-mediated therapies, and additional approaches can be developed to expand their usage. Overall, this hyperthermia-triggered drug release using CO_2 generation has demonstrated great potential for use as a systemic delivery platform for the treatment of a variety of human diseases and could be adapted to enhance other therapeutic approaches requiring specific therapeutic capabilities.

Acknowledgments

This work was supported by Basic Research Laboratory Program through the National Research Foundation of Korea (NRF) funded by the Ministry of Science, ICT and Future Planning (No. 2013R1A4A1069575). This research was also supported by Basic Science Research Program through the National Research Foundation of Korea (NRF) funded by the Ministry of Education (NRF-2013R1A1A2059167).

Appendix A. Figures with essential color discrimination

Certain figures in this article, particularly Figs. 1 and 3–6, are difficult to interpret in black and white. The full color images can be found in the on-line version, at http://dx.doi.org/10.1016/j.actbio.2015.06.019.

References

[1] T.M. Allen, P.R. Cullis, Liposomal drug delivery systems: from concept to clinical applications, Adv. Drug Deliv. Rev. 65 (2013) 36–48.
[2] E. Gentile, F. Cilurzo, L. Di Marzio, M. Carafa, C.A. Ventura, J. Wolfram, et al., Liposomal chemotherapeutics, Future Oncol. 9 (2013) 1849–1859.
[3] M. van Elk, R. Deckers, C. Oerlemans, Y. Shi, G. Storm, T. Vermonden, et al., Triggered release of doxorubicin from temperature-sensitive poly(N-(2-hydroxypropyl)-methacrylamide mono/dilactate) grafted liposomes, Biomacromolecules 15 (2014) 1002–1009.
[4] T. Ta, E. Bartolak-Suki, E.J. Park, K. Karrobi, N.J. McDannold, T.M. Porter, Localized delivery of doxorubicin in vivo from polymer-modified thermosensitive liposomes with MR-guided focused ultrasound-mediated heating, J. Control. Release 194C (2014) 71–81.
[5] S. Mura, J. Nicolas, P. Couvreur, Stimuli-responsive nanocarriers for drug delivery, Nat. Mater. 12 (2013) 991–1003.
[6] Y. Yoshizaki, E. Yuba, N. Sakaguchi, K. Koiwai, A. Harada, K. Kono, Potentiation of pH-sensitive polymer-modified liposomes with cationic lipid inclusion as antigen delivery carriers for cancer immunotherapy, Biomaterials 35 (2014) 8186–8196.
[7] T. Li, S. Takeoka, A novel application of maleimide for advanced drug delivery: in vitro and in vivo evaluation of maleimide-modified pH-sensitive liposomes, Int. J. Nanomed. 8 (2013) 3855–3866.
[8] S.H. Jung, K. Na, S.A. Lee, S.H. Cho, H. Seong, B.C. Shin, Gd(III)-DOTA-modified sonosensitive liposomes for ultrasound-triggered release and MR imaging, Nanoscale Res. Lett. 7 (2012) 462.
[9] S.R. Sirsi, M.A. Borden, State-of-the-art materials for ultrasound-triggered drug delivery, Adv. Drug Deliv. Rev. 72 (2014) 3–14.
[10] L. Paasonen, T. Sipila, A. Subrizi, P. Laurinmaki, S.J. Butcher, M. Rappolt, et al., Gold-embedded photosensitive liposomes for drug delivery: triggering mechanism and intracellular release, J. Control. Release 147 (2010) 136–143.
[11] A. Aygun, K. Torrey, A. Kumar, L.D. Stephenson, Investigation of factors affecting controlled release from photosensitive DMPC and DSPC liposomes, Appl. Biochem. Biotechnol. 167 (2012) 743–757.
[12] T. Ta, T.M. Porter, Thermosensitive liposomes for localized delivery and triggered release of chemotherapy, J. Control. Release 169 (2013) 112–125.
[13] B. Kneidl, M. Peller, G. Winter, L.H. Lindner, M. Hossann, Thermosensitive liposomal drug delivery systems: state of the art review, Int. J. Nanomed. 9 (2014) 4387–4398.
[14] J. Liu, H. Ma, T. Wei, X.J. Liang, CO_2 gas induced drug release from pH-sensitive liposome to circumvent doxorubicin resistant cells, Chem. Commun. (Camb.) 48 (2012) 4869–4871.
[15] M.F. Chung, K.J. Chen, H.F. Liang, Z.X. Liao, W.T. Chia, Y. Xia, et al., A liposomal system capable of generating CO_2 bubbles to induce transient cavitation, lysosomal rupturing, and cell necrosis, Angew. Chem. Int. Ed. Engl. 51 (2012) 10089–10093.
[16] B.Y. Choi, H.J. Park, S.J. Hwang, J.B. Park, Preparation of alginate beads for floating drug delivery system: effects of CO(2) gas-forming agents, Int. J. Pharm. 239 (2002) 81–91.
[17] K.J. Chen, H.F. Liang, H.L. Chen, Y. Wang, P.Y. Cheng, H.L. Liu, et al., A thermoresponsive bubble-generating liposomal system for triggering localized extracellular drug delivery, ACS Nano 7 (2013) 438–446.
[18] G. Haran, R. Cohen, L.K. Bar, Y. Barenholz, Transmembrane ammonium sulfate gradients in liposomes produce efficient and stable entrapment of amphipathic weak bases, Biochim. Biophys. Acta 1151 (1993) 201–215.
[19] H.D. Han, Y. Byeon, H.N. Jeon, B.C. Shin, Enhanced localization of anticancer drug in tumor tissue using polyethylenimine-conjugated cationic liposomes, Nanoscale Res. Lett. 9 (2014) 209.
[20] H.S. Kim, H.D. Han, G.N. Armaiz-Pena, R.L. Stone, E.J. Nam, J.W. Lee, et al., Functional roles of Src and Fgr in ovarian carcinoma, Clin. Cancer Res. 17 (2011) 1713–1721.
[21] J.W. Lee, H.D. Han, M.M. Shahzad, S.W. Kim, L.S. Mangala, A.M. Nick, et al., EphA2 immunoconjugate as molecularly targeted chemotherapy for ovarian carcinoma, J. Natl Cancer Inst. 101 (2009) 1193–1205.
[22] C. Lu, H.D. Han, L.S. Mangala, R. Ali-Fehmi, C.S. Newton, L. Ozbun, et al., Regulation of tumor angiogenesis by EZH2, Cancer Cell 18 (2010) 185–197.
[23] A. Fritze, F. Hens, A. Kimpfler, R. Schubert, R. Peschka-Suss, Remote loading of doxorubicin into liposomes driven by a transmembrane phosphate gradient, Biochim. Biophys. Acta 1758 (2006) 1633–1640.
[24] D. Olmeda, G. Moreno-Bueno, J.M. Flores, A. Fabra, F. Portillo, A. Cano, SNAI1 is required for tumor growth and lymph node metastasis of human breast carcinoma MDA-MB-231 cells, Cancer Res. 67 (2007) 11721–11731.